Supporting Information

Lanthanum-based nanomaterials suppress bacterial wilt in tomato: importance of particle morphology and dissolution profile

Zhenyu Wang[a,b], Tong Wang[a,b], Chuanxi Wang[a,b], Le Yue[a,b], Jing Li[a,b], Tianxi Liu[c], Yan Lv[c], Jason C. White[d], Xuesong Cao[a,b,*],Baoshan Xing[e]

[a]*Institute of Environmental Processes and Pollution control, and School of Environment and Civil Engineering, Jiangnan University, Wuxi 214122, China*

[b]*Jiangsu Engineering Laboratory for Biomass Energy and Carbon Reduction Technology, and Jiangsu Key Laboratory of Anaerobic Biotechnology, Jiangnan University, Wuxi 214122, China*

[c]*Key Laboratory of Synthetic and Biological Colloids, Ministry of Education, School of Chemical and Material Engineering, International Joint Research Laboratory for Nano Energy Composites, Jiangnan University, Wuxi 214122, China*

[d]*The Connecticut Agricultural Experiment Station, New Haven, Connecticut 06511, United States*

[e]*Stockbridge School of Agriculture, University of Massachusetts, Amherst, Massachusetts 01003, United States*

*Corresponding author:

Tel.:+86 0510 85910935; Fax:+86 0510 85910935

E-mail address: caoxuesong@jiangnan.edu.cn (Dr. Xuesong Cao)

Experiment S1. La-based NMs synthesis and characterization

$LaPO_4$ NRs and $LaPO_4$ NPs were synthesized as described by Enikeeva et al. (2020) with slight modification.[1] Briefly, 4 mL N-butanl and 8 mL Na_3PO_4 solution (0.25 M) were added into 8 mL $LaCl_3$ solution (2 mM). The pH of the mixed solution was adjusted to 6.5 using 0.1 M NaOH and HCl. The mixed solution was stirred 30 min at 400 rpm/min until forming white gelatinous substance and transferred to a 50 mL Teflon-lined stainless steel reaction kettle, with subsequent heating in the oven at 180 °C for 24 and 6 h to prepare $LaPO_4$ NRs and $LaPO_4$ NPs. The obtained white precipitates ($LaPO_4$ NRs and $LaPO_4$ NPs) were washed five times with ethanol and DI water, respectively. The synthesis method of La_2S_3 NPs was based on Rashidi *et al.* (2020) with slight modification.[2] Briefly, 1.35 g $LaCl_3{\cdot}7H_2O$ and 0.78 g $Na_2S_2O_3{\cdot}5H_2O$ were added into 10 mL PEG-400, and then the mixture was stirred at 400 rpm/min and heated at 80 °C. After 30 min reaction, the mixture was further heated in an oven at 90 °C for 24 h. The obtained sediments (La_2S_3 NPs) were washed three times with methanol, ethanol, and DI water, respectively. The preparation of La_2O_3 NPs was followed the method reported by Srivastava *et al.* (2022) with slight modification.[3] Briefly, NaOH solution (1 M) was added into 100 mL $LaCl_3{\cdot}7H_2O$ (100 mM) solution drop by drop till the pH reached at 11. The obtained white precipitate ($La(OH)_3$) was washed five times with DI water and suspended in 100 mL DI water. The $La(OH)_3$ suspension was transferred into 100 mL Teflon-lined stainless steel reaction kettle and heated at 200 °C for 8 h, with subsequent washing six times with DI water and 75% ethanol, respectively. The obtained La based NMs were freeze fried for 12 h.

The size and shape of La based NMs were observed using a transmission electron microscope (TEM, JEM-2100, Hitachi, Japan). The crystal structure of La based NMs was measured by X-ray diffraction (XRD, Bruker, Germany). The zeta potential and hydrodynamic diameter of 100 mg/L La based NMs were characterized using a Zetasizer (ZEN3600, Malvern, UK). The relative hydrophobicity of La based NMs was analyzed based on the method reported by Li *et al.* (2022).[4] Briefly, 4 mg/L Rose bengal (RB, hydrophobic dye) and Nile blue A (NB, hydrophilic dye) were prepared in phosphate buffered solution at pH 7.4. La based NMs suspensions (10 mL, 200 mg/L) were added into 10 mL dye solutions (4 mg/L) and incubated at 25 °C for 3 h, with subsequent centrifugation at 13000 rpm/min for 1 h. The concentration of RB and NB in supernatants were measured with a UV-vis spectrometer (UV-1800, SHIMADZU, Japan) at 549 and 620 nm, respectively. The relative hydrophobicity is represented by the dye adsorption ratio, calculated by the ratio of RB adsorption to NB adsorption. To assess the ion release ability of different La based NMs, 100 mg/L La based NMs suspensions were prepared and shaken at 200 rpm/min for 0, 12, 24, 48, 72, 96, and 120 h. La based NMs were removed from suspensions by centrifugation at 13000 rpm/min for 20 min and filtration with 0.22 μm membrane. In addition, the dissolution of La based NMs in the apoplastic and symplastic fluids extracted from tomato leaves were further explored. The apoplastic and symplastic fluids were extracted from tomato leaves following the method reported by Zhu et al. (2020).[5] The extracted apoplastic and symplastic fluids were ultrasonicated for 10 mins to release the biomolecular. Subsequently, La based NMs were suspended in apoplastic and symplastic fluids and

the La ions were extracted by following the above methods. The La content in supernatants was analyzed using an inductively coupled plasma mass spectrometry (ICP-MS, iCAP-TQ, Thermo Fisher, Germany).

Experiment S2. Phytohormone measurement

The phytohormone content, including SA, JA, and abscisic acid (ABA), in tomato shoots was measured according to Li *et al.* (2016).[6] Briefly, 100 mg ground fresh tomato shoots were added into a 2 mL centrifuge tube containing 1 mL ethyl acetate (10 μg/mL butylated hydroxytoluene and 7.5 mg polyvinylpyrrolidone). The mixture was immediately vortexed for 15 min, ultrasonicated in an ice water bath for 15 min, and then centrifuged (13,000 rpm, 4 °C) for 10 min. The supernatant was concentrated under nitrogen, reconstituted in 200 μL 70% methanol, vortexed for 5 min, and sonicated on ice for 10 min. The supernatant was further purified by centrifugation (12000 rpm, 4°C, 10 min) and prepared for analysis using high-performance liquid chromatography-tandem mass spectrometry (HPLC-MS/MS, Thermo Scientific, Germany) using a Waters HSS T3 chromatographic column (1.8 μm 2.1×100 mm). The mobile phase was set as A (0.01% v/v, formic acid/water) and B (0.01% v/v, formic acid/acetonitrile) using the following separation program: 0-1.5 min (95% A/5% B), 9-10 min (30% A/70% B), and 10.1-15 min (95% A/5% B). The flow rate was 0.35 mL/min. The injected sample volume was 10 μL. The MS/MS detection was performed in negative ion mode with an electrospray voltage of -3.5 kV. The capillary temperature was 320 °C and the auxiliary gas heater temperature was 350 °C. Parallel Reaction Monitoring (PRM) was used as the collection mode of MS/MS data and the resolution of MS^2 was set at 17500.

Experiment S3. Analysis of antioxidant activity and oxidative stress level

The activity of superoxide dismutase (SOD) and peroxidase (POD) in tomato shoots were analyzed according to the methods of Luo *et al.* (2021) with slight modification.[7] Firstly, 200 mg tomato leaves were homogenized in 2 mL 50 mM phosphate buffer solution (pH 7.8) under ice bath, and then centrifuged (12000 rpm, 4°C) for 30 min. The supernatant was used as the crude enzyme for activity analysis of SOD and POD. For SOD analysis, the crude enzyme was mixed with L-methionine, nitroblue tetrazole, riboflavin, and EDTA-2Na. The mixture was exposed under a fluorescent tube lamp (light intensity: 250 μmol $m^{-2}s^{-1}$) for 20 min, and then determined by a multifunctional microplate at 560 nm. SOD activity takes the amount of enzyme required to inhibit NBT photoreduction by 50% as one unit of SOD. For POD activity, the crude enzyme was mixed with 200 mM phosphate buffer solution (pH 6.0) containing guaiacol solution and 30% H_2O_2, the mixtures were immediately measured in the wavelength of 470 nm for 2min each 30s by a multifunctional microplate reader. The increase in OD value of 0.01 per minute was considered as one unit of POD. The content of malondialdehyde (MDA) can be used to reflect the degree of membrane lipid peroxidation which was assayed following the methods of Li *et al.* (2020).[8] Briefly, tomato leaves were homogenized in 0.1% (w/v) trichloroacetic acid in an ice bath, and then centrifuged (12000 rpm, 4°C) for 10 min. The supernatant was mixed with 0.5%

(m/v) thiobarbituric acid (dissolved in 10% trichloroacetic acid). After 10 min incubation in boiling water, the mixtures were rapidly cooled in an ice bath. The absorbance was measured at 532 and 600 nm by a multifunctional microplate reader. *In vivo* hydrogen peroxide (H_2O_2) detection was measured based on Ma *et al.* (2016).[9] Briefly, tomato leaves were infiltrated with 3,3'-diaminobenzidine solution (1 g/L, pH 3.8, 5 h) under vacuum, and then heated in 95% ethanol to remove the chlorophyll. Subsequently, the samples were photographed and analyzed for relative H_2O_2 levels based on the area of brown points using Image J software.

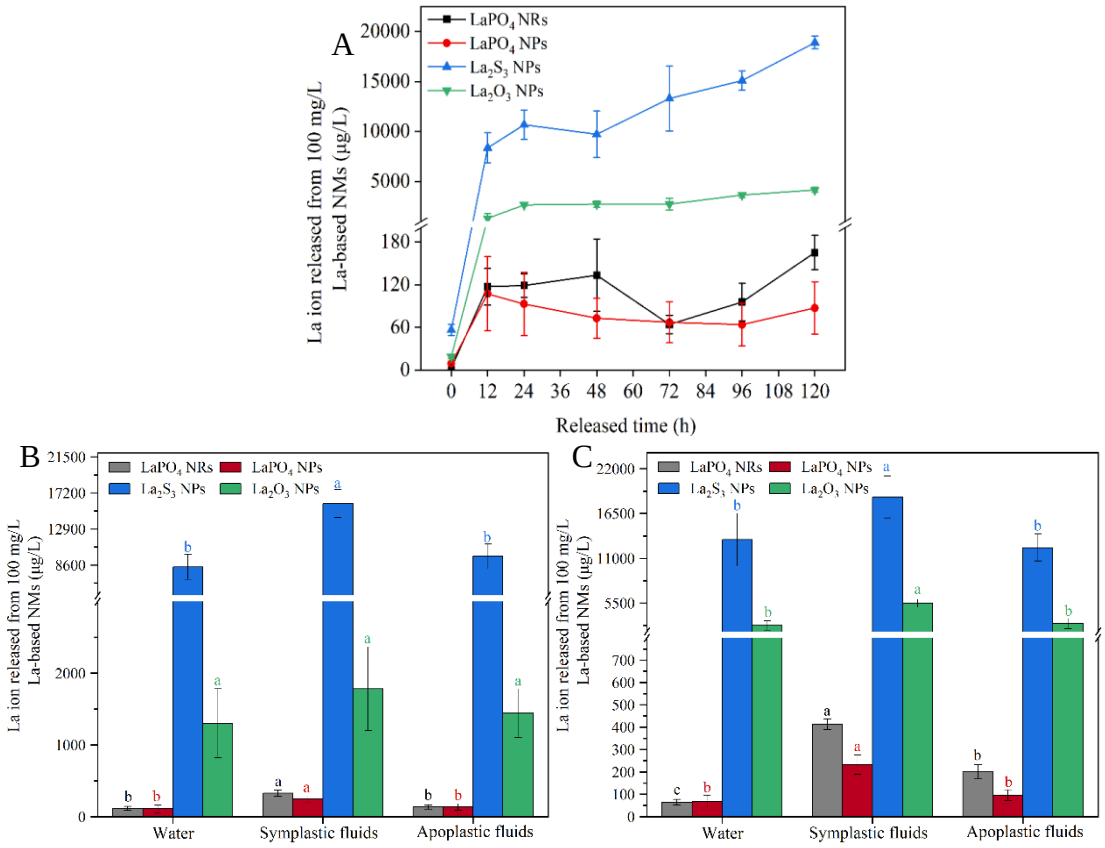

Figure S1 (A) The concentration of La ions released from 100 mg/L $LaPO_4$ NRs, $LaPO_4$ NPs, La_2S_3 NPs, and La_2O_3 NPs suspensions in DI water as function of exposure time (0, 12, 24, 48, 72, 96, and 120 h); (B) La dissolution from 100 mg/L $LaPO_4$ NRs, $LaPO_4$ NPs, La_2S_3 NPs, and La_2O_3 NPs in the apoplastic and symplastic fluids extracted from tomato leaves after 12 h exposure; (C) La dissolution from 100 mg/L $LaPO_4$ NRs, $LaPO_4$ NPs, La_2S_3 NPs, and La_2O_3 NPs in the apoplastic and symplastic fluids extracted from tomato leaves after 72 h exposure. The significant difference among different treatments is marked with different letters ($p < 0.05$, LSD, n = 6).

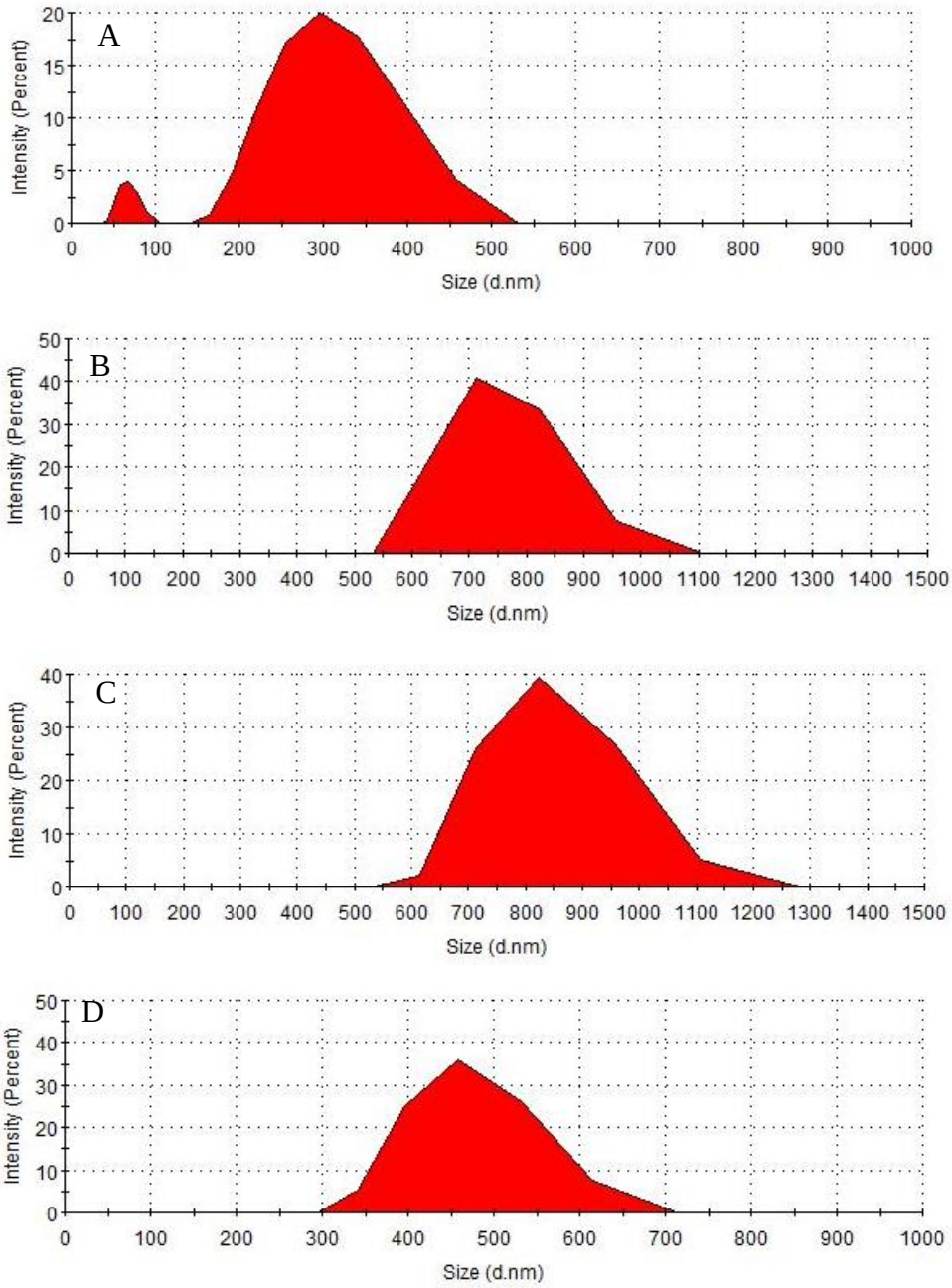

Figure S2 The size distribution diagrams of $LaPO_4$ NRs (A), $LaPO_4$ NPs (B), La_2S_3 NPs (C), and La_2O_3 NPs (D) suspension in DI water.

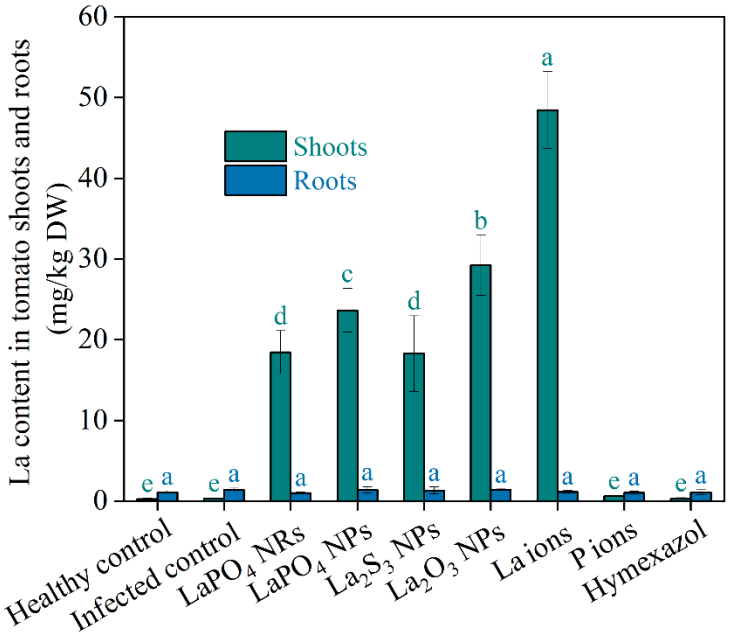

Figure S3 The content of La in tomato shoots and roots after foliar application with 100 mg/L La based nanomaterials with different formulation ($LaPO_4$ NRs, $LaPO_4$ NPs, La_2S_3 NPs, and La_2O_3 NPs), 105 mg/L $LaCl_3$ (La ions, equivalent La mass with 100 mg/L $LaPO_4$ NPs), 70 mg/L Na_3PO_4 (P ions, equivalent P mass with 100 mg/L $LaPO_4$ NPs), and 300 mg/L hymexazol. The significant difference among different treatments is marked with different letters ($p < 0.05$, LSD, n = 6).

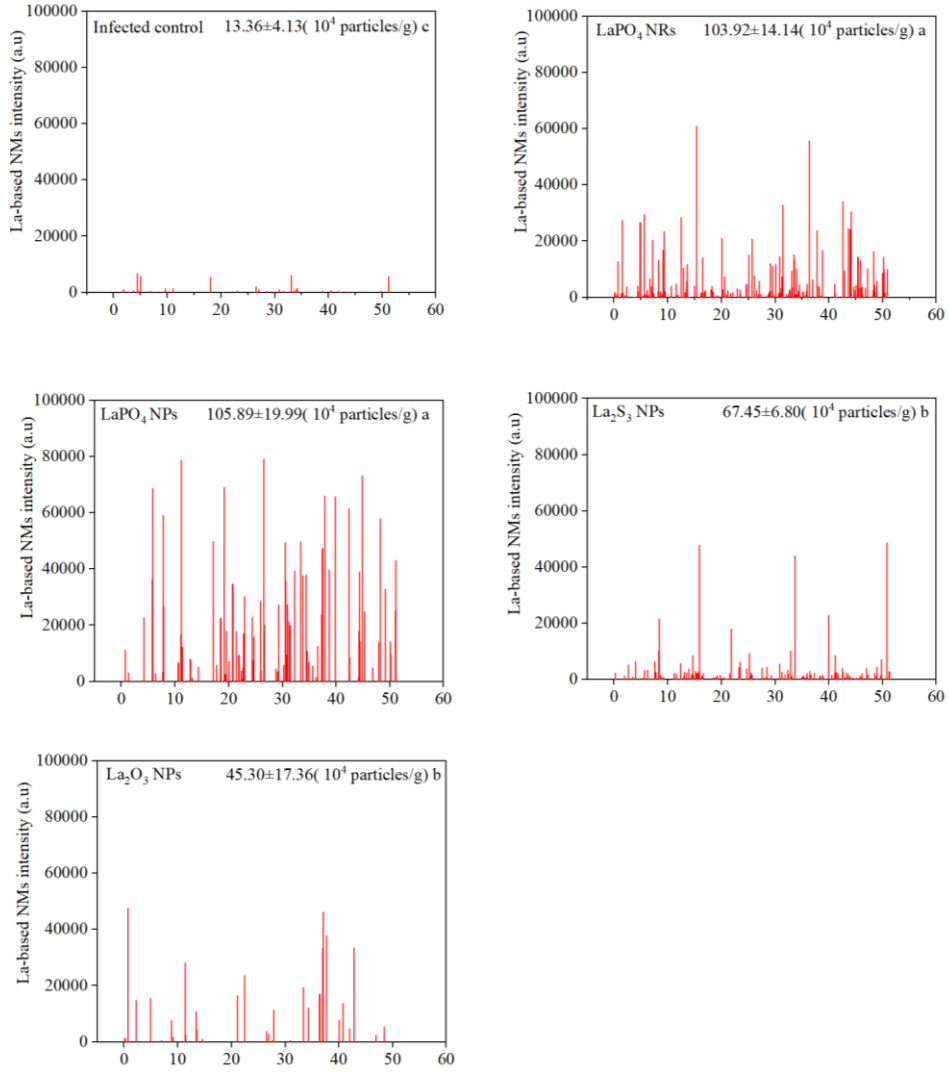

Figure S4 The content of La based NMs in tomato shoots after application with $LaPO_4$ NRs, $LaPO_4$ NPs, La_2S_3 NPs, and La_2O_3 NPs as analyzed using a sp-ICP-MS.

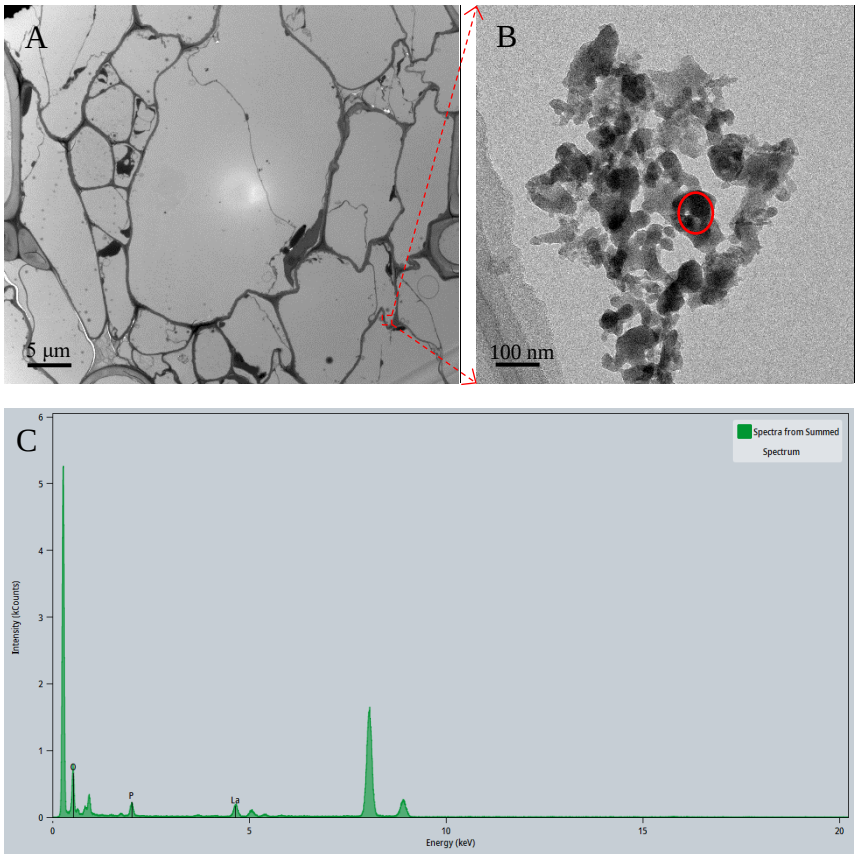

Figure S5 (A) TEM image of tomato stem after foliar application with $LaPO_4$ NPs; (B) Magnified view of the region squared in panel A; (C) EDS point scanning of the region squared in panel B.

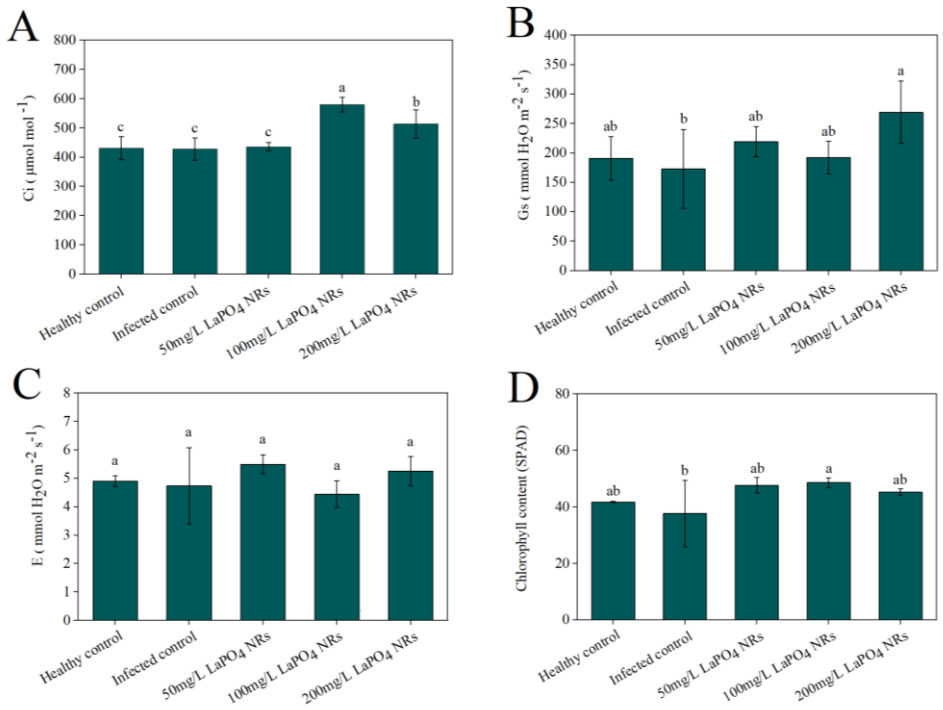

Figure S6 The photosynthetic endpoints (Ci (A), Gs (B), E (C), and chlorophyll content (D)) of *Ralstonia solanacearum* infected tomatoes after foliar application with different concentrations (50, 100, and 200 mg/L) $LaPO_4$ NRs. The significant difference among different treatments is marked with different letters ($p < 0.05$, LSD, n = 6).

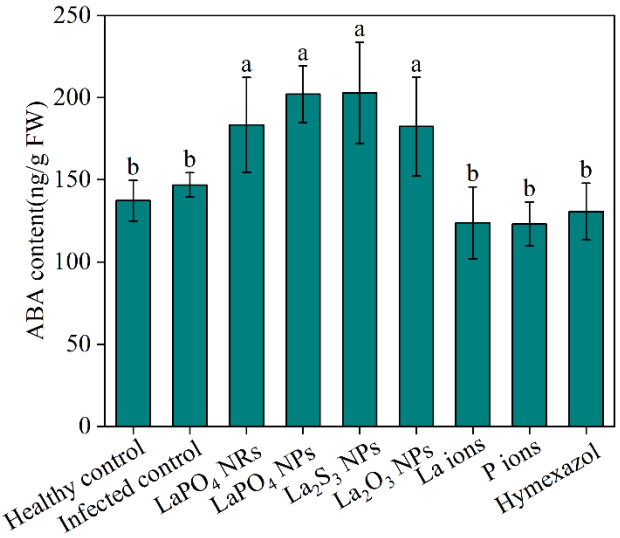

Figure S7 The concentration of ABA in pathogen infected tomato shoots as affect by foliar application with $LaPO_4$ NRs, $LaPO_4$ NPs, La_2S_3 NPs, La_2O_3 NPs, La ions, P ions, and hymexazol. The significant difference among different treatments is marked with different letters ($p < 0.05$, LSD, n = 6).

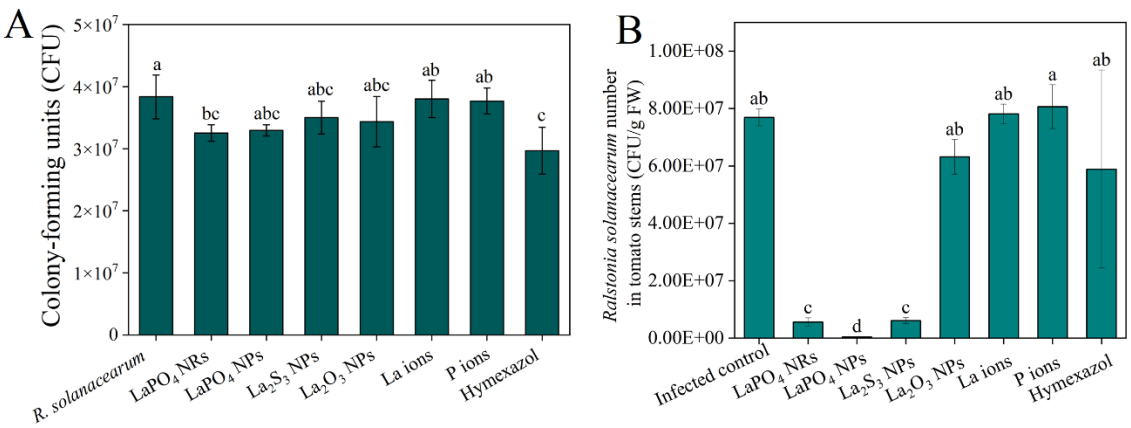

Figure S8 (A) Growth of *Ralstonia solanacearum* on PDA plates after exposure to 100 mg/L La based NMs ($LaPO_4$ NRs, $LaPO_4$ NPs, La_2S_3 NPs, and La_2O_3 NPs), 105 mg/L $LaCl_3$ (La ions, equivalent La mass with 100 mg/L $LaPO_4$ NPs), 70 mg/L Na_3PO_4 (P ions, equivalent P mass with 100 mg/L $LaPO_4$ NPs), and 300 mg/L hymexazol, respectively; (B) The abundance of *Ralstonia solanacearum* in tomato stems upon foliar application with 100 mg/L La based nanomaterials ($LaPO_4$ NRs, $LaPO_4$ NPs, La_2S_3 NPs, and La_2O_3 NPs), 105 mg/L $LaCl_3$ (La ions, equivalent La mass with 100 mg/L $LaPO_4$ NPs), 70 mg/L Na_3PO_4 (P ions, equivalent P mass with 100 mg/L $LaPO_4$ NPs), and 300 mg/L hymexazol, respectively. The significant difference among different treatments is marked with different letters ($p< 0.05$, LSD, n=6).

Table S1 Primers used in the investigation the expression of disease-related genes by an RT-qPCR approach.

Gene name	Gene symbol	Forward prime (5′-3′)	Reverse primer (5′-3′)	References
Actin-7-like	Actin	TGTCCCTATCTACGAGGGTTATGC	CAGTTAAATCACGACCAGCAAGA	1
Pathogenesis-related protein PR-5	PR5	GGCCCATGTGGTCCTACAAA	GGCAACATAGTTTAGCAGACCG	1
Pathogenesis-related protein P4	P4	GCAACAATGGGTGGTGGTTC	ACCTAAGCCACGATACCATGA	1
Jasmonic acid 2	JA2	ACGGGGACGGATAAGGTGAT	GCACCCATTCATCTAGCTTTGAA	1
Non-expressor of pathogenesis-related protein 1	NPR1	ACAAGTTGATGGCACGTCTG	CCGATTCAAGTGCTCCTCTT	2
Pathogenesis-related protein P2	PR-P2	GATGCTGACAAGCCTCTGG	TCCTGTTCCTGTGTTGGTCA	2
Pathogenesis-related protein 1	PR1	TGCAAAATGGTGGGCAAATTCA	GCCCAAGCATTAACGGCATC	2
Pathogenesis-related genes transcriptional activator PTI5	PTI5	GCGATTCGGCTAGACATGGT	CCTCGCATTCTAAAAGCCGC	3
Calmodulin 1	CAM1	GTTTCCCAATCTGCAACTTCTCT	AGTTGTGATACAACCATCTCCG	4
Calmodulin 3	CAM3	CTGTAATCGAAGAGGCGAGAAG	GTTGTAATGCAACCATCTCCG	4
Jasmonic acid-amido synthetase JAR1	JAR1	CCCACTCGAGGAAAATCTCGTA	CTGGAGTGCCATTGTGGAAT	5

Table S2. Instrumental parameters for sp-ICP-MS data acquisition

Optimized ICP-MS operating condition				
Materials	$LaPO_4$ NRs	$LaPO_4$ NPs	La_2S_3 NPs	La_2O_3 NPs
Analyte	La^{139}	La^{139}	La^{139}	La^{139}
Mass fraction (%)	0.59	0.59	0.74	0.85
Density (g/cm^3)	4.51	4.51	4.91	6.51
Dwell time (ms)	100	100	100	100
Scan time (s)	3	3	3	3
Sample flow rate (mL/min)	90	90	90	90
Mode	KED	KED	KED	KED

Table S3. The hydrodynamic diameter, zeta potential, and relative hydrophobicity of La based NMs with different morphologies and components. The significant difference among different treatments is marked with different letters ($p < 0.05$, LSD, $n = 6$).

Materials	$LaPO_4$ NRs	$LaPO_4$ NPs	La_2S_3 NPs	La_2O_3 NPs
Hydrodynamic diameter (nm)	319.2 ± 39.8^{d}	942.7 ± 31.2^{b}	1051.0 ± 146.8^{a}	570.8 ± 44.7^{c}
Zeta potential (mV)	26.1 ± 1.9^{b}	4.8 ± 0.6^{d}	12.0 ± 1.4^{c}	33.8 ± 1.0^{a}
Relative hydrophobicity	0.7 ± 0.2^{c}	6.0 ± 1.2^{a}	1.9 ± 0.2^{bc}	2.5 ± 0.5^{b}

Table S4. The content of macroelements and microelements in pathogen infected tomato shoots after foliar application with $LaPO_4$ NRs, $LaPO_4$ NPs, La_2S_3 NPs, La_2O_3 NPs, La ions, P ions, and hymexazol. The significant difference among different treatments is marked with different letters ($p < 0.05$, LSD, n = 6).

Treatments	P (g/kg)	S (g/kg)	Mg (g/kg)	Ca (g/kg)	K (g/kg)
Healthy control	1.96±0.20ab	7.07±0.80c	11.82±2.83a	40.31±11.11b	38.21±11.61a
Infected control	1.43±0.18d	7.59±1.29bc	11.95±1.43a	44.31±3.30ab	30.13±4.08ab
$LaPO_4$ NRs	2.15±0.27a	8.51±1.27ab	10.91±1.16a	42.10±3.27b	32.79±8.95ab
$LaPO_4$ NPs	2.10±0.14ab	8.73±1.21ab	12.26±1.34a	48.44±5.41ab	28.61±2.64b
La_2S_3 NPs	1.77±0.08bc	9.24±0.93a	10.0±1.16a	42.13±3.64b	29.53±4.58b
La_2O_3 NPs	1.58±0.06cd	8.50±1.03ab	12.55±2.41a	44.83±6.22ab	29.78±10.80b
La ions	1.76±0.14bc	8.16±0.76abc	11.30±1.67a	42.04±7.12b	27.33±5.77b
P ions	1.96±0.17ab	8.35±0.81ab	12.64±1.41a	51.055±7.81a	28.84±4.03b
Hymexazol	1.43±0.01d	8.25±0.97bc	11.35±0.20a	39.91±2.11b	29.83±3.72b
Treatments	Fe (mg/kg)	Zn (mg/kg)	Cu (mg/kg)	Mn (mg/kg)	Mo (mg/kg)
Healthy control	724.87±46.96ab	58.68±5.87a	9.91±1.63b	157.80±5.56a	1.93±0.19b
Infected control	535.90±114.69cd	37.28±1.71d	13.05±2.43a	118.99±7.89c	1.36±0.24c
$LaPO_4$ NRs	642.36±96.88bc	46.64±3.09bc	10.79±3.71ab	166.94±23.07a	2.02±0.21ab
$LaPO_4$ NPs	854.61±122.19a	49.83±5.49b	11.85±1.35ab	163.53±12.21a	2.33±0.29a
La_2S_3 NPs	434.68±86.98d	45.58±3.84bc	10.16±3.26ab	153.39±7.89ab	2.13±0.08ab
La_2O_3 NPs	525.67±91.90cd	48.53±14.50b	11.67±3.13ab	156.68±6.92ab	2.21±0.19ab
La ions	533.86±131.41cd	39.56±6.16cd	10.77±1.75ab	116.07±31.23c	1.45±0.32c
P ions	558.20±89.56cd	37.19±3.18d	10.29±1.84ab	132.58±17.90bc	1.46±0.43c
Hymexazol	481.96±35.51d	37.37±2.95d	13.94±1.25a	124.36±5.08c	1.48±0.15c

References

1. M.O. Enikeeva, K.M. Kenges, O.V. Proskurina, D.P. Danilovich and V.V. Gusarov, Influence of Hydrothermal Treatment Conditions on the Formation of Lanthanum Orthophosphate Nanoparticles of Monazite Structure. *Russ. J. Appl. Chem.*, 2020, **93**, 540-548.
2. H. Rashidi Nodeh, H. Sereshti, E. Beirakabad and K. Razmkhah, Synthesis and Application of Lanthanum Sulfide Nanoparticles for Removal of Tetracycline from Aqueous Media. *Int. J. Environ. Sci. Technol.,* 2020, **17**, 819-828.
3. A. Srivastava, G. Mishra, J. Singh and M.D. Pandey, A Highly Efficient Nanostructured Au@La_2O_3 Based Platform for Dopamine Detection. *Mater. Lett.,* 2022, **308**, 131231.
4. G. Li, Z. Cao, Z., K.K. Ho and Y.Y. Zuo, Quantitative Determination of the Hydrophobicity of Nanoparticles. *Anal. Chem.*, 2022, **94**, 2078-2086.
5. J. Zhu, J. Li, Y. Shen, S. Liu, N. Zeng, X. Zhan, J. C. White, J. Gardea-Torresdey and B. Xing, Mechanism of Zinc Oxide Nanoparticle Entry into Wheat Seedling Leaves. Environ. Sci.: Nano, 2020, **7**, 3901-3913.
6. Y. Li, C. Zhou, X. Yan, J. Zhang and J. Xu, Simultaneous Analysis of Ten Phytohormones in *Sargassum Horneri* by High-Performance Liquid Chromatography with Electrospray Ionization Tandem Mass Spectrometry. *J. Sep. Sci.*, 2016, **39**, 1804-1813.
7. X. Luo, X. Cao, C. Wang, L. Yue, X. Chen, H. Yang, X. Le, X. Zhao, F. Wu, Z. Wang and B. Xing, Nitrogen-doped Carbon Dots Alleviate the Damage from Tomato Bacterial Wilt Syndrome: Systemic Acquired Resistance Activation and Reactive Oxygen Species Scavenging. *Environ. Sci.: Nano,* 2021, **8**, 3806-3819.
8. Y. Li, J. Gao, X. Xu, Y. Wu, J. Zhuang, X. Zhang, H. Zhang, B. Lei, M. Zheng, Y. Liu and C. Hu, Carbon Dots as a Protective Agent Alleviating Abiotic Stress on Rice (*Oryza sativa* L.) through Promoting Nutrition Assimilation and the Defense System. *ACS Appl. Mater. Inter.,* 2020, **12**, 33575-33585.
9. C. Ma, H. Liu, H. Guo, C. Musante, S.H. Coskun, B.C. Nelson, J.C. White, B. Xing and O.P. Dhankhe, Defense Mechanisms and Nutrient Displacement in *Arabidopsis thaliana* upon Exposure to CeO_2 and In_2O_3 Nanoparticles. *Environ. Sci.: Nano*, 2016, **3**, 1369-1379.